BRIEF PAPER

Bending Loss Analysis of Chalcogenide Glass Channel Waveguides for Mid-Infrared Astrophotonic Devices

Takashi YASUI[†a)], **Jun-ichiro SUGISAKA**[†], ***Members***, ***and*** **Koichi HIRAYAMA**[†], ***Senior Member***

SUMMARY In this study, the bending losses of chalcogenide glass channel optical waveguides consisting of an As_2Se_3 core and an As_2S_3 lower cladding layer were numerically evaluated across the astronomical *N*-band, which is the mid-infrared spectral range between the 8 μm and 12 μm wavelengths. The results reveal the design rules for bent waveguides in mid-infrared astrophotonic devices.

key words: *optical waveguides, mid-infrared spectral range, chalcogenide glass, astrophotonics, beam-propagation method*

1. Introduction

Optical integrated circuits (OICs) are being widely used in astrophysics to realize high-angular-resolution and high-contrast imaging over a broad wavelength range. The application of OICs in astronomy is referred to as astrophotonics. OIC-based solutions are smaller, lighter, and less expensive than their conventional bulk-optics equivalents. In addition, they can realize functionality that is difficult or impossible to achieve by conventional solutions. Astrophotonics is important for the upcoming extremely large telescopes (ELTs) currently under construction, which will enable the detection of smaller and/or fainter objects, such as exoplanets, in detail [1].

To date, most astrophotonic instruments have been operated in the near-infrared (IR) spectral range [2]–[6]. Conversely, the mid-IR spectral range is attractive for the direct detection and characterization of an exo-earth in a habitable zone because spectral features in the mid-IR range offer signatures of important chemicals such as water, ozone, and carbon dioxide [7], [8].

The As-S-Se family of chalcogenide glasses, characterized by favorable mid-IR transmission properties [9], [10], is a promising platform for the mid-IR astrophotonic devices. Additionally, laser writing techniques [11] that can generate permanent refractive index changes for the fabrication of considerably complex optical circuits are available. In fact, the fabrication of optical waveguides consisting of an As_2Se_3 core and an As_2S_3 lower cladding layer for mid-IR astrophotonics [11], and numerical analyses of their single-mode conditions in detail [12] have been reported.

Bent waveguides are important building blocks of OICs. Although bent waveguides with small radii are vital for realizing compact and high-density OICs, losses occurring in bent waveguides increase as the bending radii decrease. In addition, a high throughput is required for astrophotonic devices because astronomical observation programs are inherently photon starved. However, to the best of our knowledge, the bending losses of chalcogenide glass optical waveguides based on the As-S-Se family in the mid-IR spectral range have not yet been characterized either experimentally or theoretically.

In this study, we performed beam-propagation analyses for bent waveguides, which consist of an As_2Se_3 core and an As_2S_3 lower cladding layer, to reveal the characteristics of bending losses across the astronomical *N*-band (8–12 μm). The results provide fundamental information for the design of high-performance astrophotonic devices operating in the mid-IR spectral range. Equivalent straight waveguides (ESWs) [13]–[17] of the bent waveguides have been analyzed using the two-dimensional finite-difference beam-propagation method (FD-BPM) [18]–[20] to estimate their loss characteristics.

2. Bent and Equivalent Straight Waveguides

Figure 1 shows the cross section of the chalcogenide glass channel waveguide, which consists of an As_2Se_3 core layer and an As_2S_3 lower cladding layer [9], [11], [12]. The refractive indices of these materials and air are denoted as n_c, n_s, and n_a, respectively. The wavelength dependencies of n_c and n_s [12], [21], [22] were considered. The refractive index change in the core layer is denoted by Δn, which is obtained by the laser writing technique using the photodarkening effect [9] to form a channel waveguide of width w_c. The effective index method (EIM) was applied to Fig. 1 to obtain equivalent two-dimensional waveguides.

Figure 2 (a) shows an equivalent two-dimensional waveguide of a bent waveguide with width of w_c and bend-

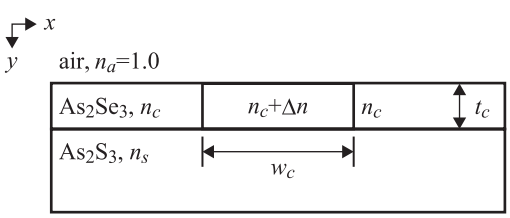

Fig. 1 Schematic of the chalcogenide glass channel waveguide.

Manuscript received May 10, 2022.
Manuscript revised June 21, 2022.
Manuscript publicized August 25, 2022.
[†]The authors are with the Faculty of Engineering, Kitami Institute of Technology, Kitami-shi, 090–8507 Japan.
a) E-mail: yasui@mail.kitami-it.ac.jp
DOI: 10.1587/transele.2022ECS6002

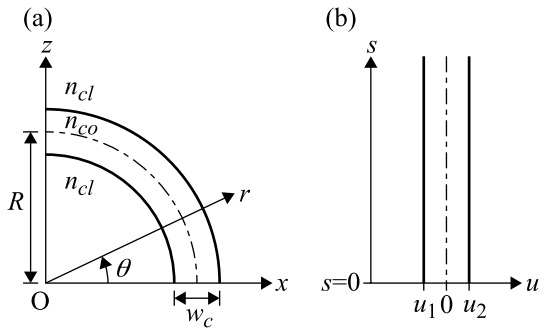

Fig. 2 (a) A two-dimensional bent waveguide, and (b) its equivalent straight waveguide. Here, $u_1 = R\ln\left(1 - \frac{w/2}{R}\right)$ and $u_2 = R\ln\left(1 + \frac{w/2}{R}\right)$.

ing radius of R. The bent waveguide can be mapped onto an ESW, as shown in Fig. 2 (b), using a conformal transformation [14]. Here, $u = R\ln\left(1 + \frac{q}{R}\right)$, $q = r - R$, $s = R\theta$, and the refractive index distribution of the ESW, $n'(u)$, is given as follows [13]–[17]:

$$n'(u) = n(q)\left(1 + \frac{q}{R}\right). \tag{1}$$

Here, $n(q)$ denotes the refractive index distribution of the bent waveguide given as follows:

$$n(q) = \begin{cases} n_{co} & \left(-\frac{w_c}{2} \le q \le \frac{w_c}{2}\right) \\ n_{cl} & (\text{otherwise}) \end{cases}, \tag{2}$$

where n_{co} and n_{cl} are, respectively, the refractive indices of the core and claddings of the two-dimensional bent waveguide evaluated by the EIM as shown in Fig. 2 (a).

3. Numerical Results

The two-dimensional FD-BPM [18]–[20] with the transparent boundary condition (TBC) [23] was employed to estimate the bending losses of the ESWs. In the BPM analyses, the fundamental mode of the original straight waveguide with a refractive index distribution of $n(q)$ is launched in ESWs at $s = 0$ [20].

First, we consider bent waveguides with $w_c = 6.5\ \mu$m, $t_c = 3.7\ \mu$m, and $\Delta n = 0.04$ in which a single mode operation is ensured for E^x and E^y modes across the astronomical N-band [12]. We note that the value of t_c is fixed at 3.7 μm throughout this study. Figure 3 illustrates the pure bend losses at the wavelengths of $\lambda_0 = 8$, 10, and 12 μm as a function of the bending radius, R. The pure bend loss was evaluated as follows [15], [24], [25]:

$$\Gamma(s) = -\frac{10}{\Delta s'}\log_{10}\left[\frac{P(s + \Delta s')}{P(s)}\right], \tag{3}$$

where $P(s)$ denotes the modal power at s, estimated by the overlap integral between the incident and propagating fields [17], and s and $s + \Delta s'$ represent the two points used to estimate the modal power. Although the losses are kept small across the range of R at $\lambda = 8\ \mu$m, they rapidly increase as R decreases at $\lambda = 12\ \mu$m because of the weaker

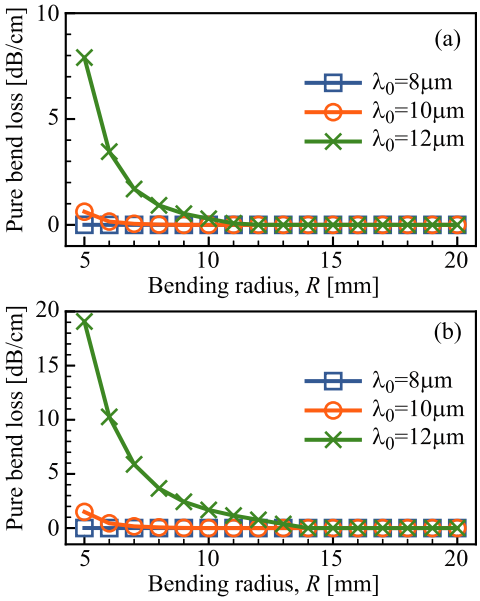

Fig. 3 Pure bend loss of bent waveguides with $w_c = 6.5\,\mu$m and $\Delta n = 0.04$ as a function of the bending radius for (a) E^x and (b) E^y modes.

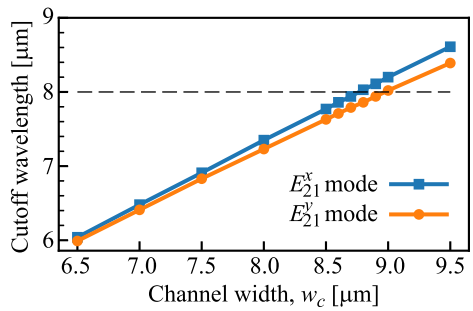

Fig. 4 Cutoff wavelength of E^x_{21} and E^y_{21} modes for a chalcogenide glass channel waveguide with $\Delta n = 0.04$ as a function of the channel width.

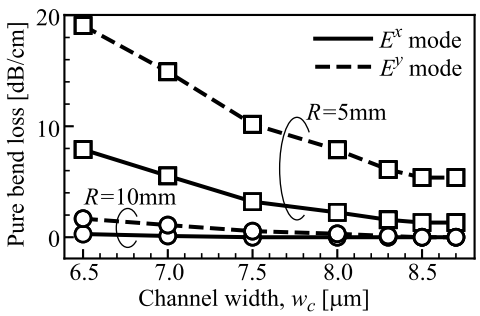

Fig. 5 Pure bend loss of bent waveguides with $\Delta n = 0.04$ at the wavelength of 12 μm for $R = 5$ and 10 mm as a function of the channel width.

confinement of the modal fields. The losses for E^y modes are larger than the ones for E^x modes because of that the effective indices of E^y modes are smaller than the ones of E^x modes for the same wavelength [12].

We considered bent waveguides with a wider channel operating in a single mode across the N-band to realize stronger confinement of the optical wave. Figure 4 illus-

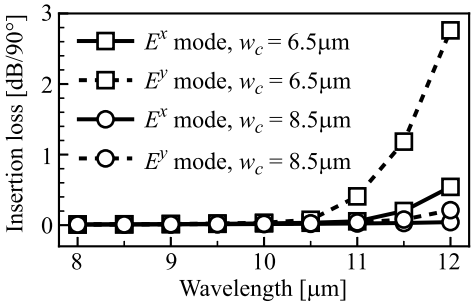

Fig. 6 Insertion loss of bent waveguides with $\Delta n = 0.04$ and $R = 10$ mm at $s = R\pi/2$ as a function of wavelength.

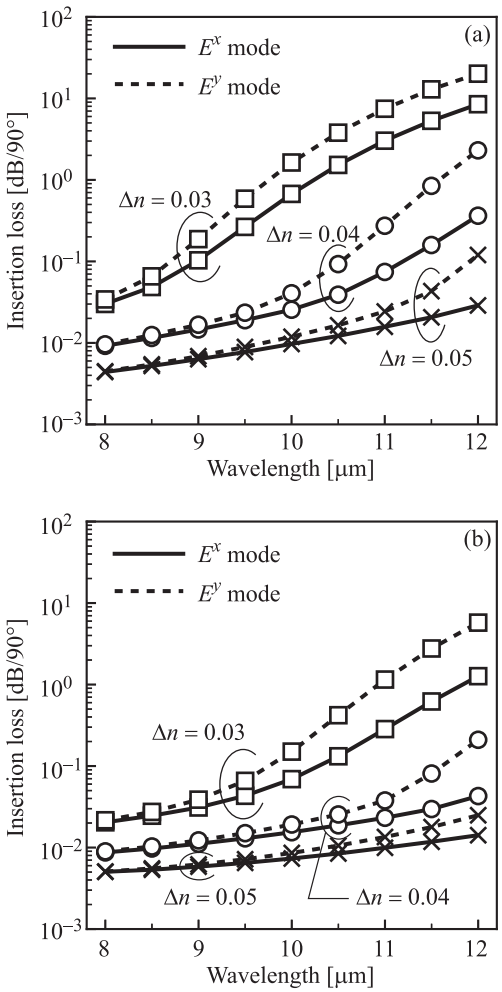

Fig. 7 Insertion loss of bent waveguides with $R = 10$ mm at $s = R\pi/2$ as a function of wavelength for (a) $w_c = 6.5\,\mu$m, (b) $w_c = 8.5\,\mu$m.

trates the cutoff wavelengths of the E^x_{21} and E^y_{21} modes of the original straight waveguide, evaluated using the EIM as a function of w_c. We observed that single mode operation is ensured for $w_c \leq 8.7$ μm for E^x mode and $w_c \leq 8.9$ μm for E^y mode. We noted that the E^x_{12} and E^y_{12} modes cannot propagate in the straight waveguide with the current value of t_c in the N-band [12]. Figure 5 shows the pure bend losses of the bent waveguides at the wavelength of 12 μm for $R = 5$ and 10 mm as a function of w_c. We observed that the loss can be suppressed by a larger w_c. Figure 6 shows the insertion losses (IL) [20], which is evaluated as

$$IL = -10\log_{10}\left[\frac{P(s)}{P(0)}\right], \tag{4}$$

of bent waveguide with $w_c = 6.5$ and 8.5 μm at the propagation distance $s = R\pi/2$ as a function of w_c. Here, $\Delta n = 0.04$ and $R = 10$ mm. The losses at longer wavelengths are suppressed by a larger w_c.

Next, we considered the dependencies of losses on the refractive index change, Δn, because the confinement of the optical wave can also be controlled by Δn. Figure 7 illustrates insertion losses of bent waveguides with $w_c = 6.5$ and 8.5 μm at $s = R\pi/2$ for $R = 10$ mm as a function of wavelength. The results for bent waveguides with $\Delta n = 0.03$, 0.04, and 0.05 are shown. We note that Δn owing to the photodarkening effect can be controlled by the exposure time, and that Δn changes as high as 0.05 [26]. In both the cases of $w_c = 6.5$ μm and 8.5 μm, we observe that the losses are suppressed by larger Δn, and that the enlargement of Δn is more effective than widening the channel to suppress the losses in the longer wavelength region. Comparing Figs. 7 (a) and (b), a smaller polarization dependency of the loss is achieved in the shorter-wavelength region for larger values of Δn and w_c. We note that the losses in Fig. 7 are indicated on the logarithmic scale to emphasize the differences between the values in the shorter wavelength range with respect to refractive index changes.

4. Conclusions

In this study, we revealed the loss characteristics of bent waveguides based on a chalcogenide glass operated in the astronomical N-band. Two-dimensional ESW models of the bent waveguides were analyzed using a two-dimensional FD-BPM. The dependence of the loss characteristics on the waveguide parameters was investigated. It was found that the loss characteristics can be drastically improved by larger values of w_c or Δn, which enhance the confinement of optical waves, particularly in the longer-wavelength region in the astronomical N-band. More accurate analyses using a three-dimensional BPM will be conducted in our future work to verify the accuracy of the cost-effective two-dimensional analysis.

Acknowledgements

This work was supported by JSPS KAKENHI Grant Number JP22K03668.

References

[1] A.N. Dinkelaker, A. Rahman, J. Bland-Hawthorn, F. Cantalloube, S. Ellis, P. Feautrier, M. Ireland, L. Labadie, and R.R. Thomson, "Astrophotonics: introduction to the feature issue," Appl. Opt., vol.60, no.19, pp.AP1–AP6, July 2021.

[2] J. Bland-Hawthorn and P. Kern, "Astrophotonics: a new era for astronomical instruments," Opt. Express, vol.17, no.3, pp.1880–1884, Feb. 2009.
[3] J. Bland-Hawthorn and S.G. Leon-Saval, "Astrophotonics: molding the flow of light in astronomical instruments," Opt. Express, vol.25, no.13, pp.15549–15557, June 2017.
[4] S. Xie, J. Zhan, Y. Hu, Y. Zhang, S. Veilleux, J. Bland-Hawthorn, and M. Dagenais, "Add–drop filter with complex waveguide bragg grating and multimode interferometer operating on arbitrarily spaced channels," Opt. Lett., vol.43, no.24, pp.6045–6048, Dec. 2018.
[5] A.S. Nayak, L. Labadie, T.K. Sharma, S. Piacentini, G. Corrielli, R. Osellame, Éric Gendron, J.-T.M. Buey, F. Chemla, M. Cohen, N.A. Bharmal, L.F. Bardou, L. Staykov, J. Osborn, T.J. Morris, E. Pedretti, A.N. Dinkelaker, K.V. Madhav, and M.M. Roth, "First stellar photons for an integrated optics discrete beam combiner at the William Herschel Telescope," Appl. Opt., vol.60, no.19, pp.D129–D142, July 2021.
[6] A. Benoît, F.A. Pike, T.K. Sharma, D.G. MacLachlan, A.N. Dinkelaker, A.S. Nayak, K. Madhav, M.M. Roth, L. Labadie, E. Pedretti, T.A. ten Brummelaar, N. Scott, V.C. du Foresto, and R.R. Thomson, "Ultrafast laser inscription of asymmetric integrated waveguide 3 dB couplers for astronomical K-band interferometry at the CHARA array," J. Opt. Soc. Am. B, vol.38, no.9, pp.2455–2464, Sept. 2021.
[7] L. Labadie and O. Wallner, "Mid-infrared guided optics: a perspective for astronomical instruments," Opt. Express, vol.17, no.3, pp.1947–1962, Feb. 2009.
[8] B.R.M. Norris, N. Cvetojevic, T. Lagadec, N. Jovanovic, S. Gross, A. Arriola, T. Gretzinger, M.A. Martinod, O. Guyon, J. Lozi, M.J. Withford, J.S. Lawrence, and P. Tuthill, "First on-sky demonstration of an integrated-photonic nulling interferometer: the GLINT instrument," Monthly Notices of the Royal Astronomical Society, vol.491, no.3, pp.4180–4193, Nov. 2019.
[9] N. Hô, M.C. Phillips, H. Qiao, P.J. Allen, K. Krishnaswami, B.J. Riley, T.L. Myers, and N.C. Anheier, "Single-mode low-loss chalcogenide glass waveguides for the mid-infrared," Opt. Lett., vol.31, no.12, pp.1860–1862, June 2006.
[10] L. Labadie, G. Martin, A. Ródenas, N.C. Anheier, B. Arezki, R.R. Thomson, H.A. Qiao, P. Kern, A.K. Kar, and B.E. Bernacki, "Advances in the development of mid-infrared integrated devices for interferometric arrays," Optical and Infrared Interferometry III, vol.8445, p.844515, Sept. 2012.
[11] L. Labadie, G. Martín, N.C. Anheier, B. Arezki, H.A. Qiao, B. Bernacki, and P. Kern, "First fringes with an integrated-optics beam combiner at 10 μm – a new step towards instrument miniaturization for mid-infrared interferometry," A&A, vol.531, p.A48, June 2011.
[12] T. Yasui, J. Sugisaka, and K. Hirayama, "Single-mode condition of chalcogenide glass channel waveguides for integrated optical devices operated across the astronomical n-band," IEICE Trans. Electron., vol.E104-C, no.8, pp.386–389, Oct. 2021.
[13] K. Petermann, "Microbending loss in monomode fibers," Electron. Lett., vol.12, no.4, pp.107–109, Feb. 1976.
[14] M. Heiblum and J. Harris, "Analysis of curved optical waveguides by conformal transformation," IEEE J. Quantum Electron., vol.11, no.2, pp.75–83, Feb. 1975.
[15] R. Baets and P.E. Lagasse, "Loss calculation and design of arbitrarily curved integrated-optic waveguides," J. Opt. Soc. Am., vol.73, no.2, pp.177–182, Feb. 1983.
[16] J. Saijonmaa and D. Yevick, "Beam-propagation analysis of loss in bent optical waveguides and fibers," J. Opt. Soc. Am., vol.73, no.12, pp.1785–1791, Dec. 1983.
[17] Y. Nito, D. Kadowake, J. Yamauchi, and H. Nakano, "Bent embedded optical waveguide with a loaded metal film for reducing a polarization dependent loss," J. Lightwave Technol., vol.31, no.19, pp.3195–3202, Oct. 2013.
[18] Y. Chung and N. Dagli, "An assessment of finite difference beam propagation method," IEEE J Quantum Electron., vol.26, no.8, pp.1335–1339, Aug. 1990.
[19] G.R. Hadley, "Wide-angle beam propagation using padé approximant operators," Opt. Lett., vol.17, no.20, pp.1426–1428, Oct. 1992.
[20] G. Pedrola, Beam Propagation Method for Design of Optical Waveguide Devices, John Wiley & Sons, 2015.
[21] B. Ung and M. Skorobogatiy, "Chalcogenide microporous fibers for linear and nonlinear applications in the mid-infrared," Opt. Express, vol.18, no.8, pp.8647–8659, April 2010.
[22] W.S. Rodney, I.H. Malitson, and T.A. King, "Refractive index of arsenic trisulfide," J. Opt. Soc. Am., vol.48, no.9, pp.633–636, Sept. 1958.
[23] G.R. Hadley, "Transparent boundary condition for beam propagation," Opt. Lett., vol.16, no.9, pp.624–626, May 1991.
[24] M. Rivera, "A finite difference BPM analysis of bent dielectric waveguides," J. Lightwave Technol., vol.13, no.2, pp.233–238, Feb. 1995.
[25] W.J. Song, G. Song, B.H. Ahn, and M. Kang, "Scalar bpm analyses of TE and TM polarized fields in bent waveguides," IEEE Trans. Antennas Propag., vol.51, no.6, pp.1185–1198, June 2003.
[26] A.C. van Popta, R.G. DeCorby, C.J. Haugen, T. Robinson, J.N. McMullin, D. Tonchev, and S.O. Kasap, "Photoinduced refractive index change in As_2Se_3 by 633nm illumination," Opt. Express, vol.10, no.15, pp.639–644, July 2002.